

# Universality of Fragmentation in the Schrödinger Dynamics of Bosonic Josephson Junctions

Kaspar Sakmann<sup>1,2</sup>, Alexej I. Streltsov<sup>2</sup>, Ofir. E. Alon<sup>3</sup>, and Lorenz S. Cederbaum<sup>2</sup>

<sup>1</sup> *Department of Physics, Stanford University, Stanford, California 94305, USA*

<sup>2</sup> *Theoretische Chemie, Physikalisch-Chemisches Institut, Universität Heidelberg, Im Neuenheimer Feld 229, D-69120 Heidelberg, Germany and*

<sup>3</sup> *Department of Physics, University of Haifa at Oranim, Tivon 36006, Israel*

(Dated: February 22, 2019)

The many-body Schrödinger dynamics of a one-dimensional bosonic Josephson junction is investigated for up to ten thousand bosons and long times. The initial states are fully condensed and the interaction strength is weak. We report on a universal fragmentation dynamics on the many-body level: systems consisting of different numbers of particles fragment to the same value at constant mean-field interaction strength. The phenomenon manifests itself in observables such as the correlation functions of the system. We explain this universal fragmentation dynamics analytically based on the Bose-Hubbard model. We thereby show that the extent to which many-body effects become important at later times depends crucially on the initial state. Even for arbitrarily large particle numbers and arbitrarily weak interaction strength the dynamics is many-body in nature and the fragmentation universal. There is no weakly interacting limit where the Gross-Pitaevskii mean-field is valid for long times.

PACS numbers: 05.60.Gg, 03.75.Kk, 05.30.Jp, 03.65.-w

Over the last few years ultracold bosons in double-well potentials have allowed the exploration of quantum many-body dynamics in a highly controllable manner. Among the phenomena predicted or observed are tunneling and self-trapping [1–5], Josephson oscillations [2–5], collapse and revival sequences [1], squeezing [6], and matter wave interferometry [7], to name a few. Of particular relevance to this work is condensate fragmentation, which has been predicted [8–12] and observed in the ground state [13], also see [6] in this context. While tunneling, self-trapping and Josephson oscillations have explanations on the mean-field level, other phenomena, e.g., collapse and revival sequences and fragmentation dynamics require many-body treatments such as the Bose-Hubbard model [1] or even the full many-body Schrödinger equation [12, 14].

In the context of bosonic Josephson junctions self-trapping – the inhibition of tunneling due to interparticle interactions – is a theoretically and experimentally well-studied phenomenon [1–4]. A two-mode Gross-Pitaevskii (GP) mean-field treatment of the junction reduces the many-body quantum dynamics to that of a classical non-rigid pendulum and self-trapping occurs from a critical value of the interaction strength onwards [1, 2]. The theory was successfully applied in the description of experiments at short time scales [3–5]. However, for longer times the dynamics can leave the realm of mean-field theory and make a many-body description necessary, see, e.g., Refs. [1, 9, 12, 15].

Here, we investigate the long-time many-body dynamics of Bose-Einstein condensates (BECs) of up to ten thousand bosons. We solve the time-dependent many-body Schrödinger equation numerically for initially fully condensed BECs in a one-dimensional bosonic Joseph-

son junction. We consider interactions that are so weak that self-trapping *cannot* occur. This Letter contains the following main results. Firstly, we report on the existence of a *universal* many-body fragmentation dynamics in bosonic Josephson junctions. Fragmentation is a basic many-boson phenomenon which is – usually – strongly dependent on the number of bosons in the system [6, 8–13]. Here we find that systems consisting of different numbers of bosons all fragment to the same value at fixed mean-field interaction strength. The appearance of such a universal many-body dynamics is unexpected and is shown here explicitly for up to 10000 bosons. The phenomenon manifests itself in observables, such as the correlation functions.

Secondly, using the Bose-Hubbard (BH) model we explain analytically how the universal fragmentation dynamics is related to the initial state and that the phenomenon occurs for arbitrarily large numbers of particles. For a whole class of condensed initial states the analytical treatment makes very accurate predictions about the fragmentation of the BEC after the collapse of the density oscillations and thus about the extent to which the many-body dynamics remains within the realm of mean-field. We thereby show that there is no limit for which GP theory remains valid at long times.

In order to compute the time-evolution of the many-body Schrödinger equation we use the MultiConfigurational Time-Dependent Hartree for Bosons (MCTDHB) method, see Ref. [3] for theory and implementation and Refs. [12, 14, 18–20] for applications. The MCTDHB method employs variational time-adaptive orbitals in the expansion of the many-boson wave function. With increasing number of orbitals the method converges to the exact many-body Schrödinger result [12, 14, 19], as was

also shown by comparison to an exactly-solvable many-body model [20]. For further details see the supplementary material [21].

It is convenient to use dimensionless units defined by dividing the Hamiltonian by  $\frac{\hbar^2}{mL^2}$ , where  $m$  is the mass of a boson and  $L$  is a length scale. The full many-body Hamiltonian then reads

$$H = \sum_{i=1}^N h(x_i) + \sum_{i<j} W(x_i - x_j), \quad (1)$$

where  $h(x) = -\frac{1}{2}\frac{\partial^2}{\partial x^2} + V(x)$  with a trapping potential  $V(x)$  and an interparticle interaction potential  $W(x - x') = \lambda_0 \delta(x - x')$ . For the potential  $V(x)$  we choose a double-well constructed by connecting two harmonic potentials  $V_{\pm}(x) = \frac{1}{2}(x \pm 2)^2$  with a natural cubic spline at  $|x| = 0.5$ . The single-particle ground  $\phi_g$  and first excited state  $\phi_u$  of  $V(x)$  are used to define left- and right-localized Wannier functions (orbitals)  $\phi_{L,R} = \frac{1}{\sqrt{2}}(\phi_g \pm \phi_u)$ . From the orbitals  $\phi_{L,R}$  the BH hopping  $J = -\langle \phi_L | h | \phi_R \rangle = 2.2334 \times 10^{-2}$  and interaction  $U = \lambda_0 \int |\phi_L|^4$  parameters, as well as the quantities  $\Lambda = U(N-1)/(2J)$  and  $t_{Rabi} = \pi/J = 140.66$  are obtained.

All one-body observables can be computed from the first-order reduced density matrix  $\rho^{(1)}(x|x') = \langle \Psi | \hat{\Psi}^\dagger(x') \hat{\Psi}(x) | \Psi \rangle = \sum_i n_i^{(1)} \alpha_i^{(1)}(x) \alpha_i^{(1)*}(x')$ , where  $\hat{\Psi}(x)$  denotes the bosonic field operator,  $|\Psi\rangle$  the many-boson wavefunction,  $\alpha_i^{(1)}(x)$  the natural orbitals, and  $n_1^{(1)} \geq n_2^{(1)} \dots$  the natural occupations with  $\sum_i n_i^{(1)} = N$ . The single-particle density is given by  $\rho(x) = \rho^{(1)}(x|x)$ . We suppress the time-argument whenever unambiguous. Bose-Einstein condensation is defined as follows: if only one eigenvalue  $n_1^{(1)} = \mathcal{O}(N)$  exists, the system is condensed [22]. If there is more than one such eigenvalue, the BEC is said to be fragmented [8–10, 23, 24]. Here, it is convenient to define the fragmentation as  $f = \sum_{i>1} n_i^{(1)}/N$ . In GP theory  $f = 0\%$  at all times, by construction. On the many-body Schrödinger level this need not be the case and  $100\% > f \geq 0\%$ . Finally we define the momentum correlation function  $g^{(2)}(k, k') = \rho(k, k')/\rho(k)\rho(k')$ , where  $\rho(k) = \langle \Psi | \hat{\Psi}^\dagger(k) \hat{\Psi}(k) | \Psi \rangle$  is the single-particle and  $\rho(k, k') = \langle \Psi | \hat{\Psi}^\dagger(k) \hat{\Psi}^\dagger(k') \hat{\Psi}(k') \hat{\Psi}(k) | \Psi \rangle$  the two-particle momentum distribution. Only for fully condensed states, i.e.  $n_1^{(1)} = N$ , the momentum correlation function is constant,  $g^{(2)}(k, k') = 1 - 1/N$ , indicating that there are no correlations between momenta, see, e.g., [24, 25]. We note that fragmentation manifests itself in correlation functions and fringe visibilities [24] and that several experiments have measured the effects of fragmentation, see for instance [6, 13, 27]. Two-particle correlations in particular were successfully measured in many recent experiments, see, e.g., [26–28].

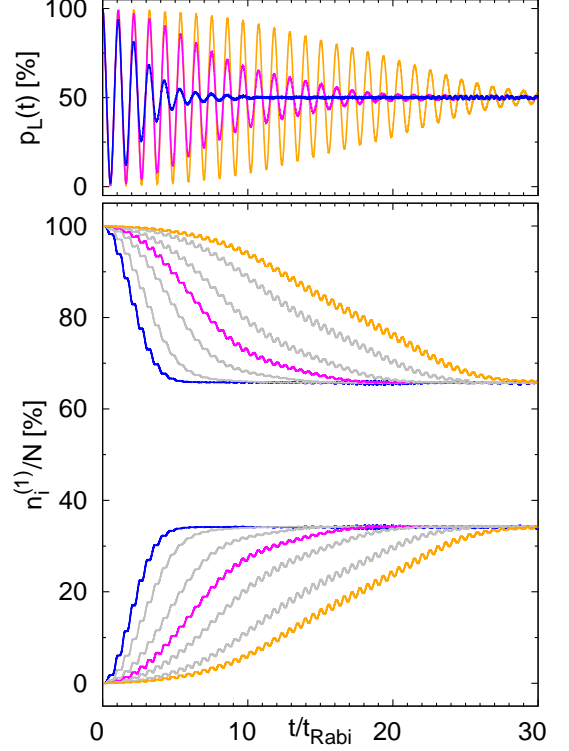


Figure 1. (color online): Universality of the many-body Schrödinger fragmentation dynamics. Shown is the probability in the left potential well  $p_L(t)$  (top) and the corresponding natural occupations  $n_i^{(1)}$  (bottom) as a function of time for different particle numbers. During the collapse of the density oscillations (top) the nature of the BEC changes from condensed to fragmented (bottom). The fragmentation reaches a plateau at  $f_{col} = 34\%$  for all particle numbers. Interaction strength:  $\lambda = 0.152$  ( $\Lambda = 1.33$ ). Particle numbers:  $N=100$  (blue), 1000 (magenta), 10000 (orange). The grey lines represent particle numbers in between,  $N=200, 500, 2000$  and 5000. All quantities shown are dimensionless.

We study the many-body dynamics for condensed initial states which are the GP ground states of the potential  $V_+(x)$ . Thus, initially the BECs are located in the left well. For each particle number  $N$  we choose the interaction strength  $\lambda_0$  such that  $\lambda = \lambda_0(N-1)$  is constant. The parameter  $\lambda$  appears in the GP equation and is known as the mean-field interaction strength. Increasing  $N$  at constant  $\lambda$  implies a decreasing interaction strength  $\lambda_0$ . In the following we fix the mean-field interaction strength at  $\lambda = 0.152$  which is equivalent to  $\Lambda = 1.33$ , i.e., well below the critical value  $\Lambda_c = 2$  for self-trapping [1, 2].

Fig. 1 (top) shows the probability in the left well  $p_L(t) = \frac{1}{N} \int_{-\infty}^0 \rho(x; t) dx$  as a function of time for  $N = 100 - 10000$  bosons. The density tunnels back and forth through the potential barrier and eventually the density oscillations collapse. With increasing particle number the collapse takes more time to occur. The collapse occurs on the many-body level, but not within GP mean-field the-

ory [1, 12]. We will therefore investigate the many-body nature of the BEC during the collapse in more detail. In Fig. 1 (bottom) the corresponding natural occupations are shown. Since the many-body wavefunction is initially condensed, there is only one natural occupation  $n_1^{(1)} = N$  at  $t = 0$ . However, as time increases a second natural orbital becomes occupied and the system fragments. The nature of the BEC changes from condensed to fragmented as the density oscillations collapse. We stress here that these results represent the many-body Schrödinger dynamics of the Hamiltonian (1). For  $N = 100$  bosons  $M = 4$  orbitals were used in the MCTDHB computation and the result is numerically exact. There is only a small quantitative difference between computations with  $M = 4$  and  $M = 2$  orbitals: until time  $t = 30t_{\text{Rabi}}$  the occupations of the third and fourth natural orbitals together stay below 0.1%. Therefore,  $M = 2$  orbitals were used in all other computations.

From Fig. 1 (bottom) we see that the fragmentation dynamics is universal: at constant mean-field interaction strength  $\lambda$  systems consisting of *different* numbers of bosons fragment to the *same* value during the collapse of the density oscillations. The two largest natural occupations reach plateaus at about  $n_1^{(1)}/N = 66\%$  and  $n_2^{(1)}/N = 34\%$ , i.e. the fragmentation after the collapse of the density oscillations settles at a value  $f_{\text{col}} = 34\%$  regardless of the number of particles involved. We recall that the GP mean-field has universal dynamics firmly built into the theory; the GP dynamics is identical for all systems with the same value of  $\lambda$ . However, here we report on a universal fragmentation dynamics which is only present on the many-body level. Fragmentation is usually strongly dependent on the number of particles in the system [8–12]. Hence, the appearance of a universal fragmentation dynamics is unexpected.

In order to establish how the universality of fragmentation manifests itself in observables we focus on the momentum correlation function  $g^{(2)}(k, k')$ . Fig. 2 shows  $g^{(2)}(k, k')$  at different times for  $N = 100$  and  $N = 1000$  bosons. The initial state is condensed and therefore  $g^{(2)}(k, k') = 1 - 1/N$ . As the system starts to fragment, correlations between particles build up and  $g^{(2)}(k, k')$  exhibits a time-varying structure. However, once the density oscillations have collapsed  $g^{(2)}(k, k')$  is nearly constant in time. It is clearly seen from the rightmost panels that the momentum correlation functions for  $N = 100$  and  $N = 1000$  bosons are the same then. Indeed, this is the case for all particle numbers considered in this work. Thus, the universality of fragmentation manifests itself unambiguously as a measurable universality of momentum correlations.

So far we have established the universality of fragmentation of the many-body Schrödinger dynamics. We will now use a simple model to show that the universality of fragmentation is a general many-body phenomenon that

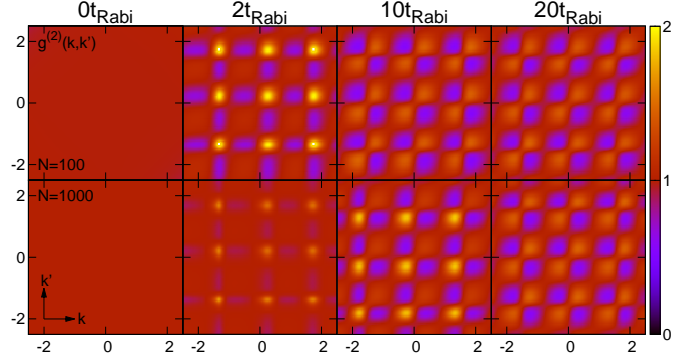


Figure 2. (color online): Universality of two-particle momentum correlations. Shown is the momentum correlation function  $g^{(2)}(k, k')$  at different times for different particle numbers. Top row:  $N = 100$  bosons. Initially the system is condensed and there are no correlations (Left panel). During the collapse of the density oscillations correlations build up (second panel). After the collapse the structure of  $g^{(2)}(k, k')$  remains practically constant in time (third and fourth panel). Bottom Row: Same as top row but for  $N = 1000$  bosons. The structure and the values of  $g^{(2)}(k, k')$  after the collapse are the same for both particle numbers. All quantities shown are dimensionless.

exists for a wide range of initial conditions and explain its origin. As a model we use the two-mode BH Hamiltonian

$$\hat{H}_{BH} = -J \left( \hat{b}_L^\dagger \hat{b}_R + \hat{b}_R^\dagger \hat{b}_L \right) + \frac{U}{2} \left( \hat{b}_L^\dagger \hat{b}_L^\dagger \hat{b}_L \hat{b}_L + \hat{b}_R^\dagger \hat{b}_R^\dagger \hat{b}_R \hat{b}_R \right), \quad (2)$$

where the operators  $\hat{b}_{L,R}$  create bosons in the orbitals  $\phi_{L,R}$  defined above. The probability in the left well reads  $p_L(t) = \frac{1}{N} \langle \hat{b}_L^\dagger \hat{b}_L \rangle(t)$  and the fragmentation of the BEC reduces here to the occupation of the second natural orbital,  $f = n_2^{(1)}/N \leq 50\%$ . We consider the family of condensed states given by

$$|\Psi_0\rangle = \frac{1}{\sqrt{N!}} \left( \sqrt{p_L(0)} \hat{b}_L^\dagger + \sqrt{p_R(0)} \hat{b}_R^\dagger \right)^N |0\rangle, \quad (3)$$

where  $p_R(0) = 1 - p_L(0)$ . We choose parameter values corresponding to the same  $\Lambda$  as above and solve the dynamics of the Hamiltonian (2). We find that for the entire family of initial states  $|\Psi_0\rangle$  with  $0 \leq p_L(0) \leq 1$ , BECs consisting of different numbers of particles fragment to the same value  $f_{\text{col}}$  during the collapse of the density oscillations. Thus, also the BH fragmentation dynamics is universal. This can be seen in Fig. 3 (left) where the fragmentation is shown as a function of time for  $N = 1000$  and 10000 bosons. The fragmentation of initial states with  $p_L(0) = 1.0$  reaches a plateau at about  $f_{\text{col}} = 32\%$ , not far from the many-body Schrödinger result  $34\%$ , see Fig. 1 (bottom). Similarly, initial states

with  $p_L(0) = 0.8$  fragment towards the value  $f_{col} = 16\%$ . Thus, the universal fragmentation dynamics is a general phenomenon which exists for a whole family of initially-condensed systems. This is also true for a wide range of interaction strengths, for details see [21].

We will now provide an analytical explanation of the universality of fragmentation based on the BH model. Consider an initial state  $|\Psi_0\rangle$  expanded in the BH eigenstates  $|E_n\rangle$  with expansion coefficients  $C_n = \langle E_n|\Psi_0\rangle$ . For a noninteracting system the  $C_n$  are binomially distributed with a width  $\sim 1/\sqrt{N}$  and the energy levels are equidistantly spaced,  $E_{n+1} - E_n = 2J$ . The system then always returns precisely to its initial state after one  $t_{Rabi}$ , regardless of its initial state. A nonzero interaction modifies the energy spectrum and shifts the distribution of the  $C_n$ . The distribution is then peaked at some  $n = n_{max}$  around those eigenstates that have an energy equal to that of the condensed initial state. The interaction causes shifts in the energy levels which let the contributions from different eigenstates go out of phase in the course of time and the system does not return precisely to its initial state anymore after one  $t_{Rabi}$ . When all contributions are completely out of phase the density oscillations average to zero and the fragmentation can be calculated. The fragmentation after the collapse of the density oscillations is then approximatively given by  $f_{col} = \min[n_{max}/N, 1 - n_{max}/N]$ , where the value of  $n_{max}$  can be determined by equating the first order expression for the BH energy eigenvalues to the energy of the initial state. Thereby, one finds

$$\frac{n_{max}}{N} = \frac{1}{2} + \frac{1}{\Lambda} - \sqrt{\frac{1}{\Lambda^2} + \frac{2\sqrt{p_L(0)p_R(0)}}{\Lambda} + \frac{3}{4} - (p_L(0)^2 + p_R(0)^2)}. \quad (4)$$

The universality of fragmentation for different particle numbers now follows directly from Eq. (4): the values for  $n_{max}/N$  and therefore for  $f_{col}$  depend on  $N$  only via the parameter  $\Lambda$  and thus all systems with the same value of  $\Lambda$  fragment to the same value  $f_{col}$ . We also note that the fragmentation of each eigenstate is given to lowest order by  $f_n = \min[n/N, 1 - n/N]$  and therefore  $f_{col} = f_{n_{max}}$ , see [21] for details.

Fig. 3 (right) shows the fragmentation  $f_n$  of each BH eigenstate as a function of  $E_n/N$  for  $N = 1000$  and  $N = 10000$  bosons. The curves for different particle numbers lie on top of each other. Also shown are the sharply peaked distributions of the expansion coefficients. By comparing the left and the right panel of Fig. 3 it is clearly seen that  $f_{col} = f_{n_{max}}$ , as predicted. The analytical prediction for  $f_{col}$  obtained from Eq. (4) is also shown here as a function of the initial state energy which is easily evaluated from Eqs. (2) and (3). The analytical results provide a good approximation to the numerical

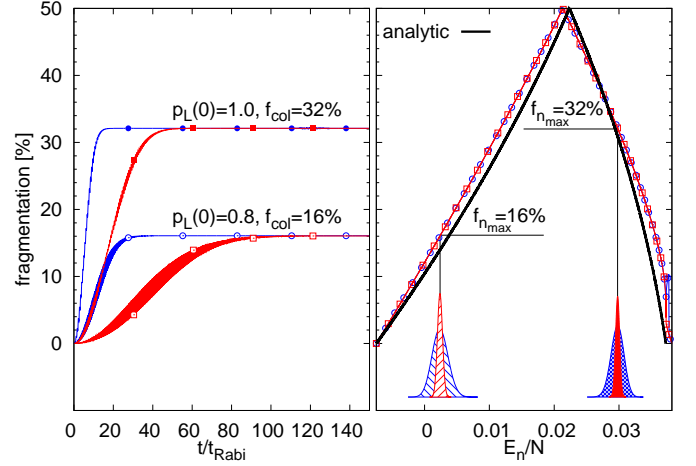


Figure 3. (color online): Universality of the Bose-Hubbard fragmentation dynamics. Interaction strength  $\lambda = 0.152$  ( $\Lambda = 1.33$ ). Left: Shown is the fragmentation dynamics of fully condensed initial states with different numbers of particles in the left well  $p_L(0)$ . Parameter values:  $N = 1000, p_L(0) = 1.0$  :  $\bullet$ ,  $N = 1000, p_L(0) = 0.8$  :  $\circ$ ,  $N = 10000, p_L(0) = 1.0$  :  $\blacksquare$ ,  $N = 10000, p_L(0) = 0.8$  :  $\square$ . The fragmentation reaches a plateau at about  $f_{col} = 32\%$  ( $f_{col} = 16\%$ ) for initial states with  $p_L(0) = 1.0$  ( $p_L(0) = 0.8$ ). Right: Shown is the fragmentation  $f_n$  of each eigenstate as a function of its energy per particle  $E_n/N$  for different particle numbers ( $N=1000$ :  $\circ$ ,  $N=10000$ :  $\square$ ) together with the analytical prediction for  $f_{col}$  (solid black). Also shown are the distributions of the expansion coefficients  $C_n$  as shaded areas ( $N=1000$ : blue,  $N=10000$ : red) peaked at  $n_{max}$  around the energies per particle  $E/N$  of the initial states (vertical lines). The fragmentation after the collapse of the density oscillation is  $f_{col} = f_{n_{max}}$  for any value of  $p_L(0)$ . The analytical prediction approximates the numerical results well. All quantities shown are dimensionless.

ones. The fragmentation  $f_{col}$  depends crucially on the initial state: from Eq. (4) it follows that, for instance, initial states with large differences in particle numbers between the left and the right well will fragment strongly, even if  $\Lambda \ll 1$ . Therefore, there cannot be a weakly interacting limit where the GP mean-field is valid at long times.

Summarizing, we have shown that there is a universal fragmentation dynamics in bosonic Josephson junctions at weak interaction strengths by solving the time-dependent many-boson Schrödinger equation. The phenomenon can be detected, for instance, through a measurement of the two-particle momentum correlation functions. We have explained the origin of this new many-body phenomenon analytically using the two-mode Bose-Hubbard model. The extent to which many-body effects become important at later times depends crucially on the initial state and there is no weakly interacting limit where the Gross-Pitaevskii mean-field is valid at long times. Further research will be devoted to the investigation of how the phenomenon can be used to produce input states for atom interferometry with definite frag-



mentation values.

Financial support by the DFG is gratefully acknowledged as is computing time at the High Performance Computing Center Stuttgart (HLRS). K.S. acknowledges funding through the Karel Urbanek Postdoctoral Research Fellowship. Discussions with Mark Kasevich are gratefully acknowledged.

- 
- [1] G. J. Milburn, J. Corney, E. M. Wright, D. F. Walls, Phys. Rev. A **55**, 4318 (1997).
  - [2] A. Smerzi, S. Fantoni, S. Giovanazzi, S. R. Shenoy, Phys. Rev. Lett. **79**, 4950 (1997).
  - [3] M. Albiez, R. Gati, J. Fölling, S. Hunsmann, M. Cristiani, M. K. Oberthaler, Phys. Rev. Lett. **95**, 010402 (2005).
  - [4] S. Levy, E. Lahoud, I. Shomroni, J. Steinhauer, Nature (London), **449**, 579 (2007).
  - [5] T. Zibold, E. Nicklas, C. Gross, and M. K. Oberthaler, Phys. Rev. Lett. **105**, 204101 (2010).
  - [6] C. Orzel, A. K. Tuchman, M. L. Fenselau, M. Yasuda, and M. A. Kasevich, Science **291**, 2386 (2001).
  - [7] T. Schumm, S. Hofferberth, L. M. Andersson, S. Wildermuth, S. Groth, I. Bar-Joseph, J. Schmiedmayer, and P. Krüger, Nature Physics **1**, 57 (2005).
  - [8] R. W. Spekkens and J. E. Sipe, Phys. Rev. A **59**, 3868 (1999).
  - [9] A. I. Streltsov, O. E. Alon, and L. S. Cederbaum, Phys. Rev. A **73**, 063626 (2006).
  - [10] E. J. Mueller, T.-L. Ho, M. Ueda, and G. Baym, Phys. Rev. A **74**, 033612 (2006).
  - [11] P. Bader and U. R. Fischer, Phys. Rev. Lett. **103**, 060402 (2009).
  - [12] K. Sakmann, A. I. Streltsov, O. E. Alon, and L. S. Cederbaum, Phys. Rev. Lett. **103**, 220601 (2009).
  - [13] S. Hofferberth, I. Lesanovsky, B. Fischer, J. Verdu, and J. Schmiedmayer, Nature Physics **2**, 710 (2006).
  - [14] K. Sakmann, A. I. Streltsov, O. E. Alon, and L. S. Cederbaum, Phys. Rev. A **82**, 013620 (2010).
  - [15] S. Raghavan, A. Smerzi, and V. M. Kenkre, Phys. Rev. A **60**, R1787 (1999).
  - [16] A. Vardi and J. R. Anglin, Phys. Rev. Lett. **86**, 568 (2001).
  - [17] A. I. Streltsov, O. E. Alon, and L. S. Cederbaum, Phys. Rev. Lett. **99**, 030402 (2007); O. E. Alon, A. I. Streltsov, and L. S. Cederbaum, Phys. Rev. A **77**, 033613 (2008); <http://MCTDHB.org>.
  - [18] K. Sakmann, A. I. Streltsov, O. E. Alon, and L. S. Cederbaum, New J. Phys. **13**, 043003 (2011).
  - [19] A. I. Streltsov, K. Sakmann, O. E. Alon, and L. S. Cederbaum, Phys. Rev. A **83**, 043604 (2011).
  - [20] A. U. J. Lode, K. Sakmann, O. E. Alon, L. S. Cederbaum, and A. I. Streltsov, Phys. Rev. A **86**, 063606 (2012).
  - [21] See supplemental material at <http://link.aps.org/supplemental/XXXX> for a comparative discussion of the MCTDHB method and the Bose-Hubbard model in the double-well system, details of the analytical model for the universality of fragmentation, an example for ten-times weaker interaction strength and a study of the time scales involved in the Schrödinger dynamics.
  - [22] O. Penrose and L. Onsager, Phys. Rev. **104**, 576 (1956).
  - [23] P. Nozières, D. Saint James, J. Phys. (France) **43**, 1133 (1982); P. Nozières, in *Bose-Einstein Condensation*, edited by A. Griffin, D. W. Snoke, and S. Stringari (Cambridge University Press, Cambridge, England, 1996).
  - [24] K. Sakmann, A. I. Streltsov, O. E. Alon, and L. S. Cederbaum, Phys. Rev. A **78**, 023615 (2008).
  - [25] M. Naraschewski and R. J. Glauber, Phys. Rev. A **59**, 4595 (1999).
  - [26] S. Fölling, F. Gerbier, A. Widera, O. Mandel, T. Gericke, and I. Bloch, Nature (London), **434**, 481 (2005).
  - [27] A. Perrin, H. Chang, V. Krachmalnicoff, M. Schellekens, D. Boiron, A. Aspect, and C. I. Westbrook, Phys. Rev. Lett. **99**, 150405 (2007).
  - [28] A. Perrin, R. Bücke, S. Manz, T. Betz, C. Koller, T. Plisson, T. Schumm, and J. Schmiedmayer, Nature Physics **8**, 195 (2012).

## SUPPLEMENTAL MATERIAL

### Schrödinger dynamics and Bose-Hubbard model in the bosonic Josephson junction system

We open the supplemental information with a comparative and deductive discussion of the theoretical methods used to explore the dynamics of the one-dimensional bosonic Josephson junction in our work.

In second quantization the Hamiltonian (1) takes on the appearance:

$$\hat{H} = \int dx \hat{\Psi}^\dagger(x) h(x) \hat{\Psi}(x) + \frac{\lambda_0}{2} \int dx \hat{\Psi}^\dagger(x) \hat{\Psi}^\dagger(x) \hat{\Psi}(x) \hat{\Psi}(x). \quad (\text{S1})$$

The theoretical approaches employed in this work, namely the Bose-Hubbard model (dimer) [S1,S2] and the the multiconfigurational time-dependent Hartree for bosons (MCTDHB) method [S3], stem from the way how the field operator

$$\hat{\Psi}(x) = \sum_j \hat{b}_j \phi_j(x) \quad (\text{S2})$$

is truncated (represented). Here  $\{\phi_j(x)\}$  is a complete set.

The Bose-Hubbard Hamiltonian (2) is obtained explicitly by restricting the field operator to a sum of only two terms

$$\hat{\Psi}(x) = \hat{b}_L \phi_L(x) + \hat{b}_R \phi_R(x). \quad (\text{S3})$$

The two ‘orbitals’ or ‘modes’  $\phi_L(x)$  and  $\phi_R(x)$  are the left- and right-localized Wannier functions as defined in the main text. They are formed by combining the delocalized, even-symmetry ground state and odd-symmetry excited state of the one-particle double-well Hamiltonian  $h(x)$ . By substituting Eq. (S3) into the many-body Hamiltonian (S1), neglecting the off-diagonal interaction terms (e.g.,  $\hat{b}_L^\dagger \hat{b}_L^\dagger \hat{b}_L \hat{b}_R$ ), and by eliminating the diagonal one-body terms (e.g.,  $\hat{b}_R^\dagger \hat{b}_R$ ), one readily arrives at the Bose-Hubbard Hamiltonian  $\hat{H}_{BH}$ , Eq. (3). From this discussion it is clear that the Bose-Hubbard Hamiltonian describes the evolution of the many-particle system between two localized *fixed-in-time* modes. The Bose-Hubbard time-dependent  $N$ -boson wavefunction takes on the form:

$$|\Psi_{BH}(t)\rangle = \sum_{n_L=0}^N C_{n_L}(t) |n_L, N - n_L\rangle, \quad (\text{S4})$$

where the time-dependent coefficients  $\{C_{n_L}(t)\}$  governing the evolution of the junction are simply obtained from the first-order equation

$$\hat{H}_{BH} |\Psi_{BH}(t)\rangle = i |\dot{\Psi}_{BH}(t)\rangle. \quad (\text{S5})$$

$\{|n_L, N - n_L\rangle\}$  are the Fock states assembled from the two ‘modes’  $\hat{b}_L^\dagger$  and  $\hat{b}_R^\dagger$ .

The dynamics governed by the Bose-Hubbard Hamiltonian occurs solely on the lowest band of the one-particle double-well problem. This emanates from Eq. (S3), namely from the retaining of the first two terms only in the expansion of the field operator in the double-well Wannier functions. It is in principle possible to retain more terms and expand the field operator in higher-band Wannier functions. This will result in a multi-band Bose-Hubbard or lattice model which, with increasing number of bands (terms in the expansion of the field operator), approaches the full many-particle Hamiltonian (S1).

Generally, many Wannier functions (Bloch bands) are needed to obtain the numerically-exact result of the Schrödinger equation, namely to faithfully represent the full many-particle Hamiltonian (S1), particularly when the time-dependent dynamics of an interacting many-body system is in need. One approach to reduce the size of the Fock space required is to employ time-adaptive orbitals rather than fixed-in-time Wannier functions (orbitals) in the expansion of the field operator:

$$\hat{\Psi}(x) = \sum_j \hat{b}_j(t) \phi_j(x, t). \quad (\text{S6})$$

The idea now is to truncate the field operator to a finite, much smaller sum of time-adaptive orbitals.

Consider  $M$  time-adaptive orbitals. When distributing the  $N$  bosons over the  $M$  orbitals the resulting time-dependent many-boson wavefunction reads:

$$|\Psi(t)\rangle = \sum_{\vec{n}} C_{\vec{n}}(t) |\vec{n}; t\rangle, \quad n_1 + n_2 + \dots + n_M = N. \quad (\text{S7})$$

In Eq. (S7) the  $\{C_{\vec{n}}(t)\}$  are the time-dependent expansion coefficients and  $\{|\vec{n}; t\rangle\}$  the time-dependent permanents (symmetrized Hartree products) built from the  $M$  time-dependent orbitals  $\{\phi_j(x, t)\}$ .

Requiring that the coefficients  $\{C_{\vec{n}}(t)\}$  and the orbitals  $\{\phi_j(x, t)\}$  of the many-boson wavefunction (S7) are determined by the time-dependent variational principle leads to the MCTDHB equations of motion [S3]. Explicitly, the MCTDHB equations of motion for the time-dependent expansion coefficients  $\{C_{\vec{n}}(t)\}$  and orbitals  $\{\phi_j(x, t)\}$  are derived by requiring stationarity of the many-body Schrödinger action functional

$$S[\{C_{\vec{n}}(t)\}, \{\phi_j(x, t)\}] = \int dt \left\{ \langle \Psi(t) | \hat{H} - i \frac{\partial}{\partial t} | \Psi(t) \rangle - \sum_{k,j=1}^M \mu_{kj}(t) [\langle \phi_k | \phi_j \rangle - \delta_{kj}] \right\}, \quad (\text{S8})$$

where  $\{\mu_{kj}(t)\}$  are time-dependent Lagrange multipliers which ensure the orthonormality of the orbitals throughout their propagation in time. The derivation is quite

lengthly but otherwise straightforward, see [S3] for the details. Here we quote the final result for the MCTDHB equations of motion which read:

$$i|\dot{\phi}_j\rangle = \hat{\mathbf{P}} \left[ h|\phi_j\rangle + \lambda_0 \sum_{k,s,l,q=1}^M \{\rho(t)\}_{jk}^{-1} \rho_{kslq} \phi_s^* \phi_l |\phi_q\rangle \right], \quad (\text{S9})$$

for the time-dependent orbitals ( $j = 1, \dots, M$ ) and

$$\mathbf{H}(t)\mathbf{C}(t) = i\dot{\mathbf{C}}(t), \quad H_{\vec{n}\vec{n}'}(t) = \langle \vec{n}; t | \hat{H} | \vec{n}'; t \rangle \quad (\text{S10})$$

for the expansion coefficients. Here,  $\hat{\mathbf{P}} = 1 - \sum_{u=1}^M |\phi_u\rangle\langle\phi_u|$  is a projector operator on the complementary space of the time-adaptive orbitals,  $\rho(t)$  the reduced one-particle density matrix,  $\{\rho_{kslq}\}$  the elements of the two-particle reduced density matrix, and  $\mathbf{C}(t) = \{C_{\vec{n}}(t)\}$  the vector of expansion coefficients. The MCTDHB method has been cast as an efficient algorithm into a software package [S4]. In practice, Eq. (S10) is simplified by a novel mapping of the configuration space [S5] which enables the efficient handling of millions of time-adaptive permanents [S4]. Furthermore, observables (like the two-particle momentum correlation function, see Fig. 2 in the main text) are directly retrieved from (the Fourier transform of) the reduced density matrices.

How many time-adaptive orbitals are needed to be taken in the truncation of expansion (S6) and, hence, in equations of motion (S9)? The answer is, as many as needed for the degree of accuracy one requires from the calculation. This number is, of course, problem dependent. The recruitment of time-adaptive orbitals allows one to achieve numerical convergence with a much smaller Hilbert space in comparison with static, time-independent orbitals [S6]. Indeed, numerical convergence to the exact time-dependent solution of the many-boson Schrödinger equation in closed [S7] and open [S8] trap potentials has been reported, as well as benchmarking against an exactly-solvable many-boson model [S6]. For more details see <http://MCTDHB.org>.

Finally, we expand on the explicit application of the MCTDHB method for the universality of fragmentation phenomenon discovered in this work. At  $t=0$ , the system is fully condensed. Its occupied orbital is the Gross-Pitaevskii ground-state in the left harmonic-potential well  $V_+(x) = \frac{1}{2}(x+2)^2$ . The initially-unoccupied orbitals at  $t=0$  are also localized in the left well and taken to be orthogonal to the first orbital and with one another (like the first few eigenfunctions of the harmonic oscillator). As the system evolves in time, the shapes of all orbitals as well as their respective occupations and the time-dependent coefficients are calculated from the MCTDHB equations of motion (S9) and (S10). Explicitly for the orbitals and in contrast to the fixed-in-time, real-valued and localized, Bose-Hubbard orbitals, the MCTDHB orbitals become complex, time-dependent functions which are generally delocalized over the two wells. In turn,

the employment of the time-adaptive orbitals takes into account the higher bands of the double-well and allows one, as discussed above, to obtained the solution to the time-dependent Schrödinger equation  $\hat{H}|\Psi(t)\rangle = i|\dot{\Psi}(t)\rangle$  to any desired accuracy.

### Details of the derivation of the universality of fragmentation

In this section we provide the details of the derivation of the analytical model for the universality of fragmentation. We begin by explaining the value of the fragmentation after the collapse of the density oscillations. To this end we evaluate the BH eigenvalues  $n_i^{(1)}$  of the first-order reduced density matrix  $\rho^{(1)}(x|x') = \sum_{i,j} \rho_{ij} \phi_j(x) \phi_i^*(x')$ . In the basis of the  $L/R$  orbitals the matrix elements  $\rho_{ij}$  can be expressed as follows:

$$\rho_{LL}(t) = \langle \Psi(t) | \hat{b}_L^\dagger \hat{b}_L | \Psi(t) \rangle = \frac{1}{2} \langle \Psi(t) | \hat{n}_g + \hat{n}_u + \hat{b}_u^\dagger \hat{b}_g + \hat{b}_g^\dagger \hat{b}_u | \Psi(t) \rangle, \quad (\text{S11})$$

$$\rho_{RR}(t) = \langle \Psi(t) | \hat{b}_R^\dagger \hat{b}_R | \Psi(t) \rangle = \frac{1}{2} \langle \Psi(t) | \hat{n}_g + \hat{n}_u - \hat{b}_u^\dagger \hat{b}_g - \hat{b}_g^\dagger \hat{b}_u | \Psi(t) \rangle, \quad (\text{S12})$$

$$\rho_{LR}(t) = \langle \Psi(t) | \hat{b}_L^\dagger \hat{b}_R | \Psi(t) \rangle = \frac{1}{2} \langle \Psi(t) | \hat{n}_g - \hat{n}_u + \hat{b}_u^\dagger \hat{b}_g - \hat{b}_g^\dagger \hat{b}_u | \Psi(t) \rangle. \quad (\text{S13})$$

Furthermore, by expanding  $|\Psi(t)\rangle$  in the BH eigenstates  $|E_n\rangle$  one finds

$$\langle \Psi(t) | \hat{b}_u^\dagger \hat{b}_g | \Psi(t) \rangle = \sum_{m \neq n} C_m^*(0) C_n(0) \langle E_m | \hat{b}_u^\dagger \hat{b}_g | E_n \rangle e^{i(E_m - E_n)t}, \quad (\text{S14})$$

$$\langle \Psi(t) | \hat{n}_{g/u} | \Psi(t) \rangle = \sum_{m,n} C_m^*(0) C_n(0) \langle E_m | \hat{n}_{g/u} | E_n \rangle e^{i(E_m - E_n)t}. \quad (\text{S15})$$

All eigenstates are parity eigenstates  $\hat{P}|E_n\rangle = \pm|E_n\rangle$ . Therefore,  $\langle E_n | \hat{b}_u^\dagger \hat{b}_g | E_n \rangle = \langle E_n | \hat{P}^\dagger \hat{P} \hat{b}_u^\dagger \hat{b}_g \hat{P}^\dagger \hat{P} | E_n \rangle = -\langle E_n | \hat{b}_u^\dagger \hat{b}_g | E_n \rangle = 0$  and the term  $m = n$  vanishes and can be left out in Eq. (S14).

For a noninteracting system the energy levels  $E_{n+1} - E_n = 2J$  are equidistantly spaced and the system always returns precisely to its initial state after a time  $t_{Rabi} = \pi/J$ , regardless of its initial state. However, the interaction modifies the energy spectrum and causes the contributions from different eigenstates to go out of phase. After a time that depends on the interaction

strength the matrix element given by Eq. (S14) averages to zero. Eqs. (S11) and (S12) then reduce to  $\rho_{LL} = \rho_{RR} = N/2$ . Similarly, only diagonal terms contribute then to Eq. (S15), and Eq. (S16) becomes

$$\begin{aligned}\rho_{LR} &\approx \frac{1}{2} \langle \Psi(t) | \hat{n}_g - \hat{n}_u | \Psi(t) \rangle \\ &\approx \frac{1}{2} \sum_{n=0}^N |C_n(0)|^2 \langle E_n | \hat{n}_g - \hat{n}_u | E_n \rangle.\end{aligned}\quad (\text{S16})$$

For weak interactions  $\langle E_n | \hat{n}_g - \hat{n}_u | E_n \rangle \approx N - 2n$ . If the number of particles is large, the distribution of the coefficients  $C_n(0)$  of the initial state is sharply peaked at  $n = n_{max}$  around the energy of the initial state. We can then replace the summation in Eq. (S16) by its value at the peak of the distribution. Thereby, we arrive at  $\rho_{LR} \approx N/2 - n_{max}$ . The two eigenvalues of the BH first-order reduced density matrix are then easily evaluated and one finds  $f_{col} = \min[n_{max}/N, 1 - n_{max}/N]$  for the fragmentation after the collapse of the density oscillations.

The value of  $n_{max}/N$  can be determined by equating the energy of the initial state

$$E = -2NJ\sqrt{p_L(0)p_R(0)} + \frac{UN(N-1)}{2}(p_L(0)^2 + p_R(0)^2). \quad (\text{S17})$$

to the first-order perturbation theory expression for the BH energy levels

$$E_n = -J(N-2n) + \frac{U}{2}(N-n)n + \frac{UN(N-1)}{4}, \quad (\text{S18})$$

where  $n = 0, \dots, N$  and solving for  $n$ . The equation is easily solved and yields (using  $N-1 \approx N$ ) Eq. (4) of the manuscript.

### Universal dynamics for weaker interactions

Here we would like to show that the universality of fragmentation phenomenon occurs over a large range of interaction strengths. For this purpose we use the Bose-Hubbard model. In particular, the dynamics remains many-body in nature and universal when the interaction strength is reduced by a factor of ten, i.e.  $\lambda = \lambda_0(N-1) = 0.0152$  ( $\Lambda = 0.133$ ). The results for the fragmentation as a function of time are shown in Fig. S1 (left). As in Fig. 3 the dynamics is shown for the two condensed initial states with  $p_L(0) = 1.0$  and  $p_L(0) = 0.8$ . As for stronger interaction we find here that BECs with different particle numbers fragment to the same value in the course of the dynamics. Condensed initial states with all particles in the left well,  $p_L(0) = 1.0$ , now fragment to about  $f_{col} = 48.3\%$  which is higher than for stronger interaction. Likewise, condensed initial states

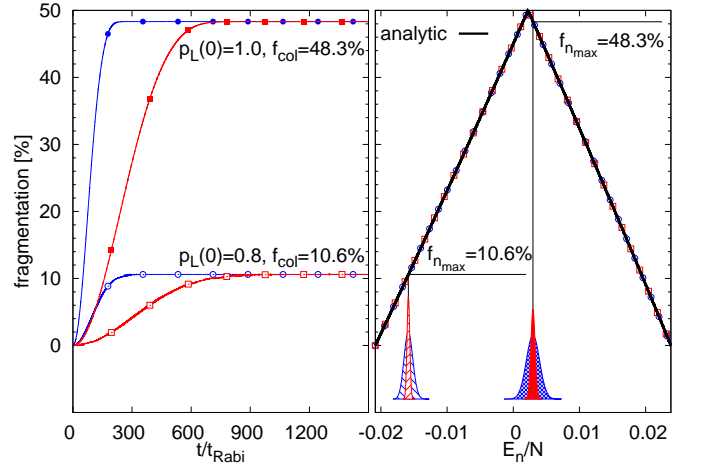


Figure S1. (color online). Universality of the Bose-Hubbard fragmentation dynamics for weaker interaction. Interaction strength is ten-times smaller,  $\lambda = 0.0152$  ( $\Lambda = 0.133$ ). All other parameter values are the same as in Fig. 3. Left: The fragmentation reaches here a plateau at about  $f_{col} = 48.3\%$  for initial states with  $p_L(0) = 1.0$  and about  $f_{col} = 10.6\%$  for  $p_L(0) = 0.8$ . These values are, respectively, higher and lower than for stronger interaction. Note the different, slower time scale. Right: analogous to Fig. 3 one finds  $f_{col} = f_{n_{max}}$  for any value of  $p_L(0)$ , as shown here for  $p_L(0) = 1.0$  and  $p_L(0) = 0.8$ . The analytical prediction for  $f_{col}$  (solid black) provides an excellent approximation to the numerical results. All quantities shown are dimensionless.

with  $p_L(0) = 0.8$  fragment to about  $f_{col} = 10.6\%$  which is lower than for stronger interaction. The time scale is roughly ten times larger for this interaction strength. Nevertheless even for large particle numbers the BECs eventually fragment to the same value. Thus, the BH dynamics is universal and many-body in nature over a wide range of interaction strengths.

The values to which the BECs fragment can be predicted from the initial state in the same way as for stronger interaction. For the initial states discussed above we find that the analytical predictions on the basis of Eq. (4) agree with the numerical results to three(!) significant digits. Thereby, the fragmentation after the collapse of the density oscillations can again be predicted from the initial state. As expected the agreement is now much better due to the weaker interaction strength. This is clearly visible in Fig. S1 in complete analogy to Fig. 3 of the main text.

### Logarithmic scaling of the fragmentation time

Here we briefly discuss the time scales involved in the Schrödinger fragmentation dynamics shown in Fig. 1. We define the fragmentation time  $T_{frag}$  as the first time at which a certain fragmentation  $f$  is reached. Fig. S2 shows the fragmentation time  $T_{frag}$  as a function of  $N$ .



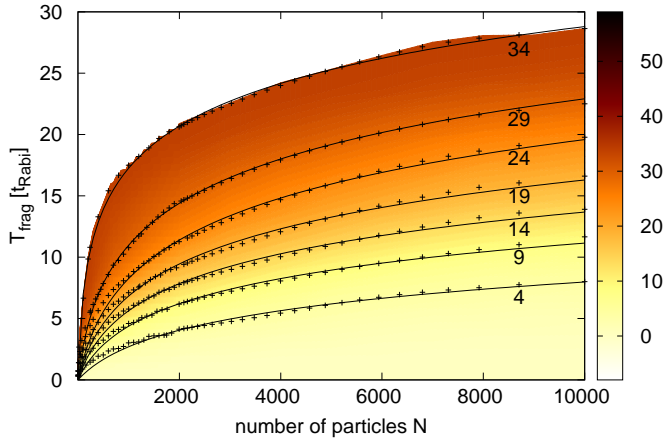


Figure S2. (color online): Many-body Schrödinger fragmentation times. Shown are the times  $T_{frag}$  that are needed to reach a given fragmentation  $f$  as a function of the number of bosons for the same parameters as in Fig. 1. The fragmentation values (crosses) are well described by a logarithmic fit function (lines), here shown for the values  $f = 4\%, 9\%, \dots, 34\%$ . This logarithmic dependence of  $T_{frag}$  on the number of particles implies the breakdown of GP mean-field theory even in the limit of large particle numbers. See text for details. All quantities shown are dimensionless.

Clearly,  $T_{frag}$  increases with  $N$ . For any value of the fragmentation,  $T_{frag}$  is well described by a fit to the function  $T(N) = a \ln(1 + bN)$ , as is shown here for the values  $f = 4\%, 9\%, \dots, 34\%$ . Thus,  $T_{frag}$  grows logarithmically with  $N$ . Consequently, the fragmentation does not decrease or even disappear in the limit of large  $N$ .

Even for  $N = 10000$  bosons the fragmentation rises to about 10% in less than a dozen  $t_{Rabi}$ . As GP theory does not allow BECs to fragment at all,  $T_{frag}$  defines a measure for the breakdown of mean-field theory. Thus, we find here a logarithmic dependence of the breakdown of mean-field theory on the number of particles within the time-dependent many-body Schrödinger equation. We note that a logarithmic breakdown of mean-field theory has been reported earlier based on the BH model [S9].

- 
- [S1] D. Jaksch, C. Bruder, J. I. Cirac, C. W. Gardiner, and P. Zoller, Phys. Rev. Lett. **81**, 3108 (1998).
  - [S2] R. Gati and M. K. Oberthaler, J. Phys. B **40**, R61 (2007).
  - [S3] A. I. Streltsov, O. E. Alon, and L. S. Cederbaum, Phys. Rev. Lett. **99**, 030402 (2007); O. E. Alon, A. I. Streltsov, and L. S. Cederbaum, Phys. Rev. A **77**, 033613 (2008).
  - [S4] A. I. Streltsov, K. Sakmann, A. U. J. Lode, O. E. Alon, and L. S. Cederbaum, *The Multiconfigurational Time-Dependent Hartree for Bosons Package*, version 2.1, Heidelberg (2011).
  - [S5] A. I. Streltsov, O. E. Alon, and L. S. Cederbaum, Phys. Rev. A **81**, 022124 (2010).
  - [S6] A. U. J. Lode, K. Sakmann, O. E. Alon, L. S. Cederbaum, and A. I. Streltsov, Phys. Rev. A **86**, 063606 (2012).
  - [S7] K. Sakmann, A. I. Streltsov, O. E. Alon, and L. S. Cederbaum, Phys. Rev. Lett. **103**, 220601 (2009).
  - [S8] A. U. J. Lode, A. I. Streltsov, K. Sakmann, O. E. Alon, and L. S. Cederbaum, Proc. Natl. Acad. Sci. USA **109**, 13521 (2012).
  - [S9] A. Vardi and J. R. Anglin, Phys. Rev. Lett. **86**, 568 (2001).